



Pyridone derivatives carrying radical moieties: Hydrogen-bonded structures, magnetic properties, and metal coordination

Ueda, Mikio

Mochida, Tomoyuki

Mori, Hatsumi

(Citation)

Polyhedron, 52:755-760

(Issue Date)

2013-05-22

(Resource Type)

journal article

(Version)

Accepted Manuscript

(URL)

<https://hdl.handle.net/20.500.14094/90001816>



Pyridone derivatives carrying radical moieties: Hydrogen-bonded structures, magnetic properties, and metal coordination[‡]

Mikio Ueda^{a,†}, Tomoyuki Mochida^{a, b,*}, Hatsumi Mori^c

^a*Department of Chemistry, Faculty of Science, Toho University, Miyama, Funabashi, Chiba 274-8510, Japan*

^b*Department of Chemistry, Graduate School of Science, Kobe University, Rokkodai, Nada, Hyogo 657-8501, Japan*

^c*Institute for Solid State Physics, The University of Tokyo, Kashiwanoha, Kashiwa, Chiba 277-8581, Japan*

Abstract

Pyridone derivatives carrying radical moieties were prepared, namely a nitronyl nitroxide derivative 5-(4',4',5',5'-tetramethylimidazoline-3'-oxide-1'-oxyl)-2(1*H*)-pyridone (**1**) and a verdazyl derivative 1,5-dimethyl-3-[2(1*H*)-pyridone]-6-oxoverdazyl (**2**). In the solid state, **1** and **2** form, via N–H···O intermolecular hydrogen bonds between the pyridone moieties, a zigzag one-dimensional chain structure and a cyclic dimer structure, respectively. These compounds exhibit antiferromagnetic intermolecular interactions. Mononuclear metal complexes [M(hfac)₂(**1**)₂] (M = Cu^{II}, Mn^{II}; hfac = bis(hexafluoroacetylacetonate)) were prepared in which *trans*-[M(hfac)₂] are coordinated with the carbonyl oxygen of the pyridone ligands. Cyclic hydrogen bonds between the mononuclear units result in the formation of one-dimensional chains. Small antiferromagnetic (for Cu^{II}) and ferromagnetic (for Mn^{II}) exchange interactions between the metal ion and the ligands were observed.

Keywords: Pyridone; Nitronyl nitroxide; Verdazyl; hydrogen bond; Metal complexes; Magnetic properties; Crystal structures

[‡]Dedicated to Alfred Werner on the 100th Anniversary of his Nobel Prize in Chemistry in 1913.

*Corresponding author. Tel./fax: +81-78-803-5679, *E-mail address*: tmochida@platinum.kobe-u.ac.jp
(T. Mochida).

[†]Present address: Wayo Konodai Girls' High School, Ichikawa, Chiba.

1. Introduction

Pyridone derivatives are versatile molecules in supermolecular chemistry and their hydrogen-bonded aggregation patterns have attracted attention [1]. For example, 2(1*H*)-pyridones produce hydrogen-bonded structures such as cyclic dimers, one-dimensional chains, and three-dimensional assemblies (Fig. 1). Pyridone derivatives can assume keto and enol tautomeric forms as well as the deprotonated form (Fig. 2). Since the establishment for the basis of coordination chemistry by Werner [2], varying the ligand components and their coordination modes has been the main strategy to explore novel structures and functionalities of coordination compounds. Thanks to their varied coordination modes, pyridone derivatives act as highly versatile ligands that have produced a number of metal cluster complexes [3]. In particular, the use of such ligands has led to the understanding of metal-metal multiple bonds [3a] and to the production of single-molecule magnets [3b,4].

Magnetism of molecular compounds has attracted continued interest over the last few decades [5]. Stable organic radicals, such as nitronyl nitroxides [6] and verdazyls [7], have proven to be useful building blocks for molecular magnets, and the magnetic properties of metal complexes with such radical ligands have been extensively investigated [5,8]. We have also reported on several metal complexes with these radical ligands [9]. Based on the features of pyridones mentioned above, we were intrigued by the use of pyridone derivatives for the construction of hydrogen-bonded and metal-coordinated magnetic assemblies [10]. Several organic radicals carrying hydrogen-bonding sites have been reported to date [11]. In this study, we investigated the structures and magnetic properties of pyridone-substituted nitronyl nitroxide and verdazyl radicals,

5-(4',4',5',5'-tetramethylimidazoline-3'-oxide-1'-oxyl)-2(1*H*)-pyridone (**1**) and 1,5-dimethyl-3-[2(1*H*)-pyridone]-6-oxoverdazyl (**2**) (Fig. 3), with the structure of **1** having been briefly mentioned in a conference proceeding [12]. In this paper, we also report the structures and properties of mononuclear metal complexes $[M(\text{hfac})_2(\mathbf{1})_2]$ ($M = \text{Cu}^{\text{II}}, \text{Mn}^{\text{II}}$; hfac = bis(hexafluoroacetylacetonate)). We previously reported the structures and magnetic properties of a dinuclear copper complex and a mononuclear palladium complex with **1** [9b] that have different coordination modes from the present complexes.

2. Results and Discussion

2.1. Preparation

Compounds **1** and **2** were prepared from the corresponding aldehyde precursors according to standard procedures [6,7]. The reaction of **1** and $[M(\text{hfac})_2]$ ($M = \text{Cu}^{\text{II}}, \text{Mn}^{\text{II}}$) in methanol afforded mononuclear metal complexes $[M(\text{hfac})_2(\mathbf{1})_2]$. No crystalline metal complexes were obtained from **2**, partly because the radical molecule was less stable. In the IR spectra, the C=O stretching bands of **1**, **2**, and $[M(\text{hfac})_2(\mathbf{1})_2]$ in the solid state were observed at 1667 cm^{-1} , 1653 cm^{-1} , and 1646 cm^{-1} , respectively. These are comparable to that in 2-pyridone (1650 cm^{-1}), indicating that the keto form predominates in the crystals, as is confirmed by crystallography discussed in the following sections.

2.2. Crystal structure and magnetic property of **1**

Compound **1** crystallized in the monoclinic space group $P2_1/a$. The nitronyl nitroxide moiety and the pyridone ring in the molecule are twisted from planar by about 22° . The molecules form a zigzag chain structure via hydrogen bonds between the pyridone moieties, as shown in Fig. 4a. The hydrogen bond distance (N...O distance: $2.680(4)\text{ \AA}$) is significantly shorter than those observed in other pyridone derivatives [1,13]. Further, the hydrogen-bonded chains stack along the *a*-axis, and the molecules are weakly dimerized with an intermolecular N–O...O–N distance of $3.763(4)\text{ \AA}$. The dimeric molecular arrangement is shown in Fig. 4b.

The temperature dependence of the magnetic susceptibility of **1** is shown in the form of a χ vs. T

plot (Fig. 5). The χT value at 300 K corresponds to the value of $S = 1/2$ non-interacting spins (0.375 emu K mol⁻¹). With decreasing temperature, the χT value shows a decrease from temperatures of about 50 K and below. Considering the dimeric molecular arrangement, the magnetic data were analyzed on the basis of a singlet-triplet model using the Bleaney-Bowers equation ($H = -2JS_1 \cdot S_2$) [14], with the best-fit parameters of $J/k_B = -6.23$ K and $\theta = -0.61$ K obtained, where J is the intradimer interaction and θ is the mean-field intermolecular interaction.

2.3. Crystal structure and magnetic property of **2**

Compound **2** crystallized in the monoclinic space group $C2/c$, with the verdazyl and pyridone rings in the molecule twisted from planar by about 15°. In the crystal, **2** forms a cyclic hydrogen-bonded dimer, as shown in Fig. 6a. The hydrogen-bond distance (N...O distance: 2.751(4) Å) is typical of pyridone derivatives. The packing diagram is shown in Fig. 6b. The radical molecules assemble into head-to-tail arrangements and form a stair-like structure along the a -axis, while, as shown by dashed lines in Fig. 6b, there is dimer overlap between the verdazyl rings. The centroid-centroid distance between the verdazyl rings is 3.39 Å.

The temperature dependence of the magnetic susceptibility of **2** is shown in Fig. 5. The χT value at 300 K (0.365 emu K mol⁻¹) is close to the value of $S = 1/2$ non-interacting spins (0.375 emu K mol⁻¹). With decreasing temperature, the χT values first steadily decreased and then decreased rapidly at temperatures below around 130 K. This strong antiferromagnetic interaction is ascribable to the dimerization of the verdazyl ring. Similar to the case of **1**, the magnetic data were analyzed on the basis of the singlet-triplet model, which yielded the intradimer exchange coupling of $J \sim -100$ K. The concentration of the Curie impurities was estimated to be 1.5%.

2.4. Structures and magnetic properties of $[M(hfac)_2(\mathbf{1})_2]$

Isomorphous $[M(hfac)_2(\mathbf{1})_2]$ ($M = Cu^{II}$ and Mn^{II}) crystallized in the $P-1$ space group. The crystal structure of the Cu^{II} complex is shown in Fig. 7. The nitronyl nitroxide moiety and the pyridone ring in the radical ligands are twisted by about 20° from planar. The complexes form centrosymmetric

trinuclear units in which two radical molecules are coordinated to the *trans* positions of the metal ion by the carbonyl oxygen of the pyridone moiety. Furthermore, the trinuclear units interact via dimeric intermolecular hydrogen bonds between the pyridone moieties, forming one-dimensional chain structures. More particularly, the carbonyl oxygen in the ligand interacts both with the metal ion and the NH hydrogen. The hydrogen bond distances (N...O distances) for the copper and manganese complexes are 2.897(3) Å and 2.936(3) Å, respectively. In the Cu^{II} complex, the bond lengths around the metal center are Cu–O_{pyridone} = 2.310(2) Å and Cu–O_{hfac} = 1.958(2) Å. The axial bond length is longer owing to Jahn-Teller distortion. In the Mn^{II} complex, the bond lengths are Mn–O_{pyridone} = 2.197(2) Å, and Mn–O_{hfac} = 2.130(2) Å and 2.132(3) Å. The trifluoromethyl groups in the hfac ligands are disordered over two sites in both complexes, with an occupancy of about 6:4.

The temperature dependence of the χT values for the Cu^{II} and Mn^{II} complexes is shown in Fig. 8. In the Cu^{II} complex, the χT value at 300 K was 1.09 emu K mol⁻¹, which corresponds to three isolated $S = 1/2$ spins (1.125 emu K mol⁻¹). With decreasing temperature, the χT value remained nearly constant down to 10 K and then decreased. The data were analyzed on the basis of a linear three-spin model ($H = -2J S_1 \cdot S_M + S_M \cdot S_2$) [15]. The exchange coupling between the metal center and the radical was determined to be $J/k_B = -0.35$ K ($g = 2.00$). In the Mn^{II} complex, the χT value at 300 K was 5.00 emu K mol⁻¹, which is close to the theoretical value for uncorrelated two $S = 1/2$ spin and an $S = 5/2$ for octahedrally coordinated Mn^{II} (5.12 emu K mol⁻¹). With decreasing temperature, the χT value remained constant down to 60 K and then gradually increased, reaching a maximum at 6 K and then rapidly decreased. Fitting of the data on the basis of the linear three-spin model gave $J/k_B = +0.78$ K ($g = 2.00$), indicating the presence of small ferromagnetic coupling in the mononuclear unit.

The magnetic interactions were interpreted based on the consideration of the magnetic orbitals. In the Cu^{II} complex (Fig. 9a), the orthogonality of the singly occupied magnetic orbital $d_{x^2-y^2}$ and the $2p$ orbital of the carbonyl oxygen may be responsible for the antiferromagnetic interaction when one considers the spin polarization in the radical ligand. In the Mn^{II} complex, however, d_{xz} and d_{yz} of the five magnetic orbitals overlap with the $2p$ orbital of the carbonyl oxygen of **1** (Fig. 9b), which may thus be responsible for the ferromagnetic interaction. The small J values for the present complexes are

ascribed to very small spin densities on the pyridone rings. Much stronger exchange couplings are reported for ligands with aminoxyl radicals owing to the more extensive spin delocalization onto the ligating sites: the metal-ligand magnetic interactions in mononuclear complexes of $[M(hfac)_2]$ with bis{4-(*N*-*tert*-butyl-*N*-oxyamino)pyridine} are $J/k_B = +60.4$ K for $M = Cu^{II}$ and -12.4 K for $M = Mn^{II}$ [15a].

We reported previously that **1** assumes the deprotonated form in the dinuclear Cu^{II} complex and the enol form in the mononuclear Pd^{II} complex, coordinating via the nitrogen atom [9b]. The formation of the keto form in the $[M(hfac)_2]$ complexes has further demonstrated the variability of the coordination modes of the ligand. In all of the complexes studied, magnetic interactions within the units are weak. In terms of spin delocalization, **2** is more advantageous than **1**, but the ligand produced no metal complexes. In these complexes, the radical moieties have additional coordination ability, which may further lead to higher dimensional coordination structures when other additional metal ions are used.

3. Conclusion

Pyridone-substituted nitronyl nitroxide and verdazyl radicals were prepared and their structures and magnetic properties investigated. These radicals exhibited one-dimensional chain structures and dimeric structures via hydrogen bonds. The $[M(hfac)_2]$ complexes ($M = Cu, Mn$) with the nitroxide radical ligand produced mononuclear complexes, which were further hydrogen bonded to form chain structures in the crystals. The mononuclear units, regarded as linear three-spin systems, exhibited very weak magnetic couplings between the metal center and the radical ligands. The verdazyl ligand, for which larger spin delocalization is expected, produced no metal complexes. The pyridone moieties in the $[M(hfac)_2]$ complexes assumed the keto form, whereas the ligand assumed the enol form and the deprotonated form in the previously reported complexes [9b]. Thus, a series of open-shell molecular assemblies were prepared that reflect the variety of hydrogen-bonding modes and coordination modes obtainable with pyridone ligands.

4. Experimental

4.1. General

2,3-Bis(hydroxyamino)-2,3-dimethylbutane [16] and carbonic acid bis(1-methylhydrazide) [17] were prepared according to literature methods. Other chemicals were commercially available.

¹H-NMR spectra were measured on a JEOL ECP400 spectrometer. Infrared spectra were recorded on a JASCO FT-IR 230 spectrometer using KBr pellets. Elemental analyses were performed using a Yanagimoto MT-3 CHN analyzer. ESR spectra were measured on a JEOL JES-TE100 spectrometer (X-band microwave unit). The magnetic susceptibilities were measured using a Quantum Design MPMS-2 SQUID susceptometer in the temperature range 2–300 K under a magnetic field of 1 T.

4.2. Preparation of **1**

4.2.1. 2-Benzyloxy-5-bromopyridine

Benzyl alcohol (1.68 g, 15.5 mmol) was added to a suspension of sodium hydride (0.61 g, 15.2 mmol, 60% dispersion in oil) in DMF (6 mL) cooled with an ice bath. After stirring the mixture for 30 min at room temperature, a DMF solution (10 mL) of 2,5-dibromopyridine (3.08 g, 13.0 mmol) was added dropwise to the solution. After stirring for 5 h, acetic acid (3 mL) was added dropwise to the solution at 0 °C and stirred for 30 min. The solution was then diluted with toluene (30 mL), washed with water (20 mL), before 5% aqueous NaHCO₃ (80 mL) was added. The organic layer was dried over magnesium sulfate, filtered, and the solvent evaporated under a reduced pressure. The crude product was purified by column chromatography (silica gel, eluent: CHCl₃:hexane = 1:2). 2-benzyloxy-5-bromopyridine was obtained as a colorless solid (3.41 g, yield 99%). Recorded analytical data were in accordance with literature values [18].

4.2.2. 6-Benzyloxypyridine-3-carbaldehyde

n-Butyl lithium (9.0 mL, 1.59 M solution in *n*-hexane) was added to a THF solution (20 mL) of 2-benzyloxy-5-bromopyridine (3.40 g, 12.9 mmol) at –78 °C. After stirring for 30 min, anhydrous DMF (1.25 mL, 16.3 mmol) was added dropwise to this solution. After stirring for 1 h at –78 °C, water (3.0 mL) was added and the solution left at room temperature overnight. The reaction product was extracted by dichloromethane, washed with water, and dried over magnesium sulfate. The crude

product was purified by column chromatography (silica gel, eluent: CHCl_3 :hexane = 1:1). After evaporation of the solvent, a yellow oil of 6-benzyloxy pyridine-3-carbaldehyde was obtained (2.66 g, yield 97%). $^1\text{H-NMR}$ (400 MHz, CDCl_3) δ 9.97 (1H, s), 8.65 (1H, s), 8.08 (1H, d, $J = 10.7$ Hz), 7.47–7.34 (5H, m), 6.90 (1H, d, $J = 8.8$ Hz), 5.49 (2H, s).

Palladium carbon (0.18 g, 10 wt% on activated carbon) was added to a methanol solution (30 mL) of thus obtained 6-benzyloxy pyridine-3-carbaldehyde (2.66 g, 12.5 mmol). Under hydrogen atmosphere, the suspension was stirred at room temperature overnight. Water (30 mL) was then added to the reaction mixture, filtered, and the solvent evaporated under a reduced pressure. Recrystallization from chloroform/hexane gave a white powder of 6-benzyloxy pyridine-3-carbaldehyde (0.88 g, yield 58%). $^1\text{H-NMR}$ (400 MHz, DMSO) δ 9.59 (1H, s), 8.23 (1H, s), 7.79 (1H, d, $J = 9.7$ Hz), 6.45 (1H, d, $J = 9.3$ Hz).

4.2.3. 5-(4',4',5',5'-Tetramethylimidazoline-3'-oxide-1'-oxyl)-2(1H)-pyridone (**1**)

A methanol solution (40 mL) of 6-benzyloxy pyridine-3-carbaldehyde (475 mg, 3.86 mmol), 2,3-bis(hydroxyamino)-2,3-dimethylbutane (625 mg, 4.22 mmol), and 2,3-bis(hydroxyamino)-2,3-dimethylbutane sulfonate (40 mg, 0.16 mmol) was stirred at room temperature. After stirring for 4 d, the solvent was removed by evaporation. The crude solid was suspended in dichloromethane (40 mL), to which an aqueous solution (10 mL) of NaIO_4 (970 mg, 4.53 mmol) was added slowly. After stirring for 10 min, the organic layer was separated, dried with MgSO_4 , and evaporated under a reduced pressure. The crude product was purified by column chromatography (silica gel, eluent: acetone:diethyl ether = 1:2). The product was recrystallized from dichloromethane/hexane to give blue crystals of **1** (512 mg, yield 53%). ESR (in CH_2Cl_2): $a_{\text{N}} = 0.78$ mT (2 N) at $g = 2.008$; FT-IR (KBr): ν/cm^{-1} 1667(C=O); Anal. Calcd for $\text{C}_{12}\text{H}_{16}\text{O}_3\text{N}_3$: C, 57.59; H, 6.44; N, 16.79. Found: C, 57.62; H, 6.42; N, 16.63.

4.3. Preparation of **2**

4.3.1. 1,5-Dimethyl-3-[2(1H)-pyridone]-1,2,4,5-tetrazane 6-oxide

A methanol solution (15 mL) of 5-formyl-2(1*H*)-pyridone (215 mg, 1.7 mmol) was added dropwise to a warm solution of carbonic acid bis(1-methylhydrazide) (254 mg, 2.2 mmol) in methanol (35 mL). After the solution was refluxed for 24 h, the solvent was evaporated under a reduced pressure, before the residue was washed with chloroform and air dried. Pale yellow powder (372 mg, yield 95%). FT-IR (KBr): ν/cm^{-1} 3242s, 1664s, 1589s, 1432s, 1390s; $^1\text{H-NMR}$ (400 MHz DMSO): δ 11.56 (br, s, 1H), 7.52 (dd, 1H), 7.33 (s, 1H), 6.32 (d, 1H), 5.67 (d, 2H), 4.72 (t, 1H), 2.92 (s, 6H) ppm; Anal. Calcd for $\text{C}_9\text{H}_{13}\text{N}_5\text{O}_2$: C, 48.42; H, 5.87; N, 31.37. Found: C, 48.19; H, 5.92; N, 31.06%.

4.3.2. 1,5-Dimethyl-3-[2(1*H*)-pyridone]-6-oxoverdazyl (**2**)

A solution of NaIO_4 (334 mg, 1.6 mmol) in water (20 mL) was added to a methanol solution (20 mL) of 1,5-dimethyl-3-[2(1*H*)-pyridone]-1,2,4,5-tetrazane 6-oxide (315 mg, 1.4 mmol) prepared as above. The solution immediately turned deep red, and after 30 min of stirring, the product was extracted with dichloromethane. The solvent was removed by evaporation, to which diethylether was added and the solution stored in a refrigerator for several days. The product was filtered, washed with diethyl ether, and then dried to produce dark red crystals (104 mg, yield 33%). FT-IR (KBr): $\nu_{\text{max}}/\text{cm}^{-1}$ 3442w, 1682s, 1653s 1628m, 1442s; $\lambda_{\text{max}}/\text{nm}$ (DMF) 273, 320sh, 338sh, 394, 417, 529; ESR (in DMF): $a_{\text{N}} = 0.56$ mT (4 N) at $g = 2.005$; Anal. Calcd for $\text{C}_9\text{H}_{10}\text{N}_5\text{O}_2$: C, 49.09; H, 4.58; N, 31.80. Found: C, 48.89; H, 4.49; N, 31.92%.

4.4. Preparation of $[\text{M}(\text{hfac})_2]$ complexes ($M = \text{Cu}, \text{Mn}$) with **1**

$[\text{Cu}(\text{hfac})_2(\mathbf{1})_2]$ was prepared as follows. A methanol solution (1 mL) of **1** (2 mg, 0.008 mmol) was added to a methanol solution (1 mL) of bis(hexafluoroacetylacetonate)copper(II) (19 mg, 0.004 mmol). After standing the solution at room temperature for several days, deep blue needle crystals of $[\text{Cu}(\text{hfac})_2(\mathbf{1})_2]$ were obtained. FT-IR (KBr): ν/cm^{-1} 3132(NH), 1646(C=O); Anal. Calcd for $\text{C}_{34}\text{H}_{34}\text{O}_{10}\text{N}_6\text{F}_{12}\text{Cu}$: C, 41.75; H, 3.50; N, 8.59. Found: C, 41.72; H, 3.54; N, 8.63. $[\text{Mn}(\text{hfac})_2(\mathbf{1})_2]$, which was prepared by the same method, gave deep blue needle crystals. IR (KBr): ν/cm^{-1} 3132(NH), 1646(C=O); Anal. Calcd for $\text{C}_{34}\text{H}_{34}\text{O}_{10}\text{N}_6\text{F}_{12}\text{Mn}$: C, 42.12; H, 3.53; N, 8.67. Found: C, 41.85; H, 3.55;

N, 8.59.

4.5. X-ray Crystal Structure Analyses

The X-ray data for **1** and [Cu(hfac)₂(**1**)₂] were collected on a Rigaku AFC-5S four circle diffractometer, and those for **2** and [Mn(hfac)₂(**1**)₂] on a Rigaku Mercury CCD diffractometer, using MoK α radiation. Crystallographic parameters are listed in Table 1. The structures were solved by direct methods and refined using the teXsan software package [19] for **2** and SHELX-97 [20] for the other compounds. The hydrogen atoms were placed at idealized positions and allowed to ride on the relevant heavier atoms. ORTEP-3 [21] was used to generate the molecular graphics.

Appendix A. Supplementary data

CCDC 882833–882836 contain the supplementary crystallographic data for **1**, **2**, [Cu(hfac)₂], and [Mn(hfac)₂]. These data can be obtained free of charge via <http://www.ccdc.cam.ac.uk/conts/retrieving.html>, or from the Cambridge Crystallographic Data Centre, 12 Union Road, Cambridge CB2 1EZ, UK; fax: +44-1223-336-033; or e-mail: deposit@ccdc.cam.ac.uk.

Acknowledgments

We sincerely thank Dr. Ulrich Schatzschneider and Prof. Eva Rentschler (Max-Planck-Institut für Strahlenchemie, Germany) for theoretical estimation of the magnetic properties in the early stage of this study. We thank Yusuke Funasako (Kobe University) for crystallographic analysis, Dr. Hideaki Suzuki (Tokyo University) for his help with SQUID measurements, and Mr. Masaru Nakama (Crayonsoft, Inc.) for providing a Web-based database system. This work was supported financially by KAKENHI (No. 23110719) and was carried out under the Visiting Researcher's Program of the Institute for Solid State Physics, the University of Tokyo.

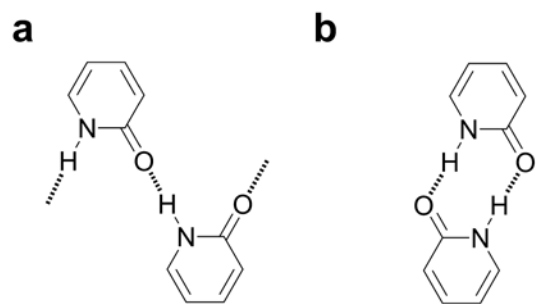


Fig. 1. Hydrogen-bonded structures of pyridone in the solid state: (a) cyclic dimer and (b) one-dimensional chain.

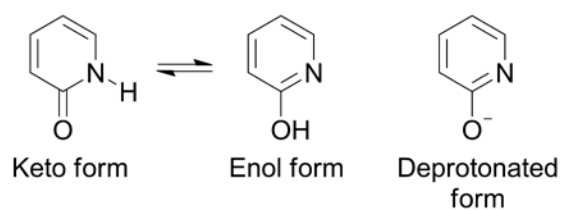


Fig. 2. The keto, enol, and deprotonated forms of 2(1*H*)-pyridone.

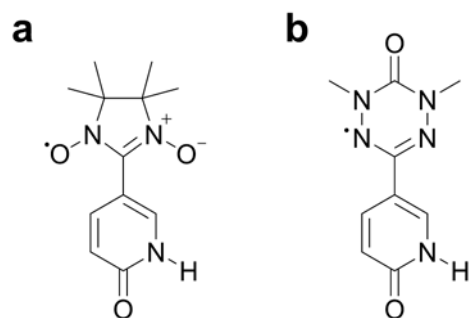


Fig. 3. Structural formulae of (a) **1** and (b) **2**.

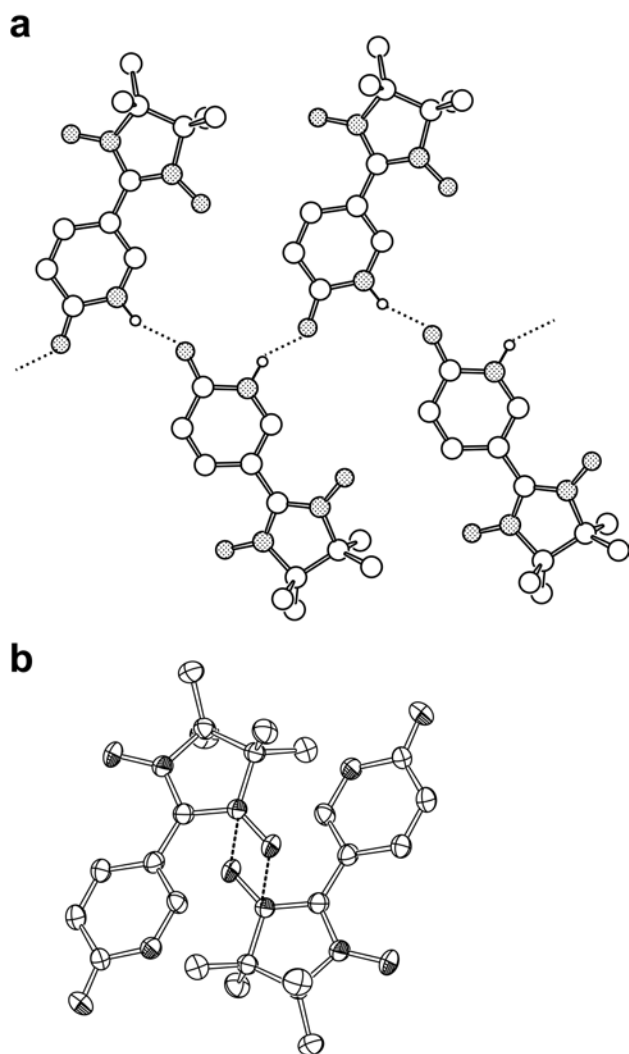


Fig. 4. Molecular arrangement of **1** in the solid state. (a) One-dimensional hydrogen-bonded structure. Dashed lines represent hydrogen bonds. (b) Overlapping mode within the molecular stack. Dashed lines indicate the shortest intermolecular N-O...O-N distances. Hydrogen atoms have been omitted, except for the NH hydrogens in (a).

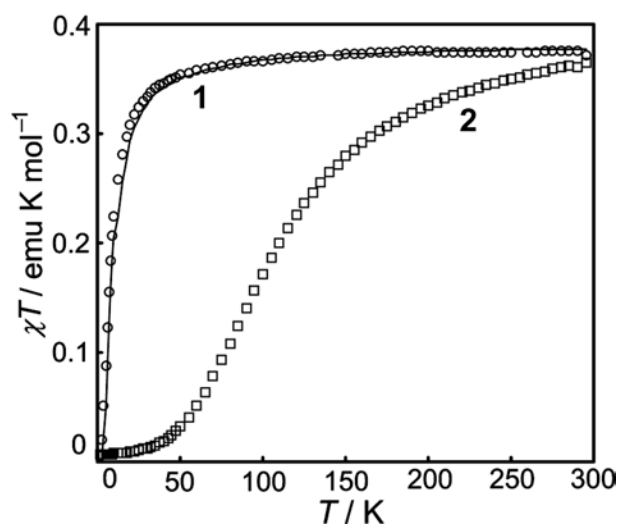


Fig. 5. Temperature dependence of the magnetic susceptibilities of **1** and **2**, plotted in the form of χT vs. T .

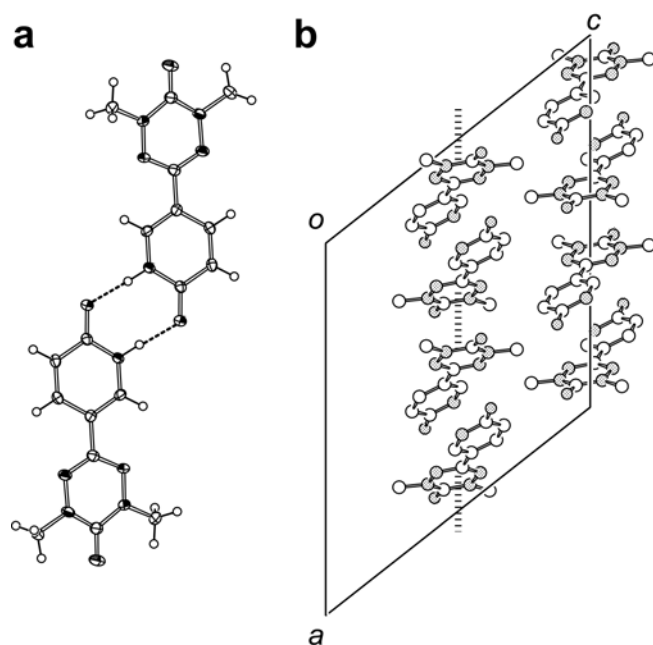


Fig. 6. Molecular arrangement of **2** in the solid state. (a) The cyclic dimer unit. Dashed lines represent hydrogen bonds. (b) Packing diagram viewed along the b -axis. Dashed lines represent the dimer formation between radical moieties.

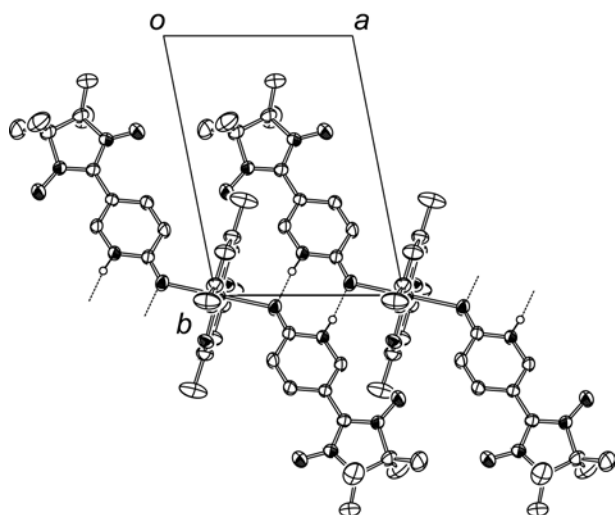


Fig. 7. Molecular structure of $[\text{Cu}(\text{hfac})_2(\mathbf{1})_2]$ in the solid state. Dashed lines represent hydrogen bonds. The trifluoromethyl groups have been omitted for clarity. Hydrogen atoms, except for the NH hydrogens, have been omitted.

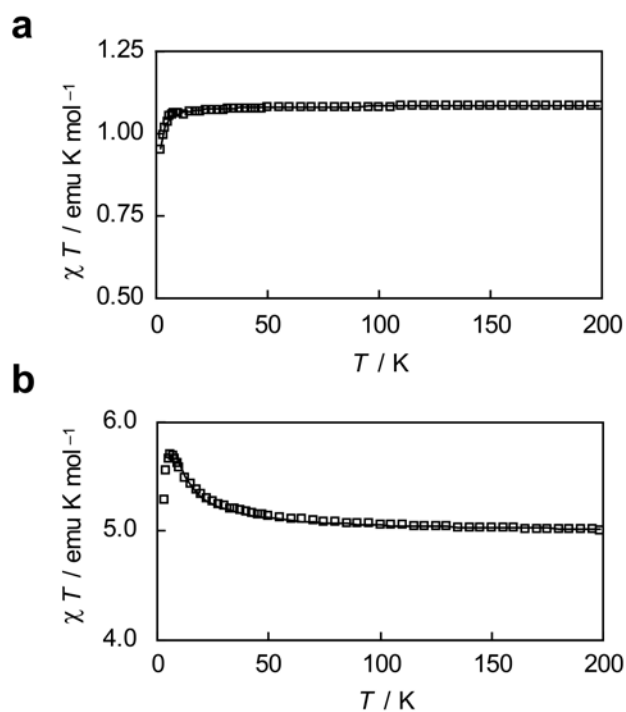


Fig. 8. Temperature dependence of the magnetic susceptibilities of (a) $[\text{Cu}(\text{hfac})_2(\mathbf{1})_2]$ and (b) $[\text{Mn}(\text{hfac})_2(\mathbf{1})_2]$, represented in the form of χT vs. T plots.

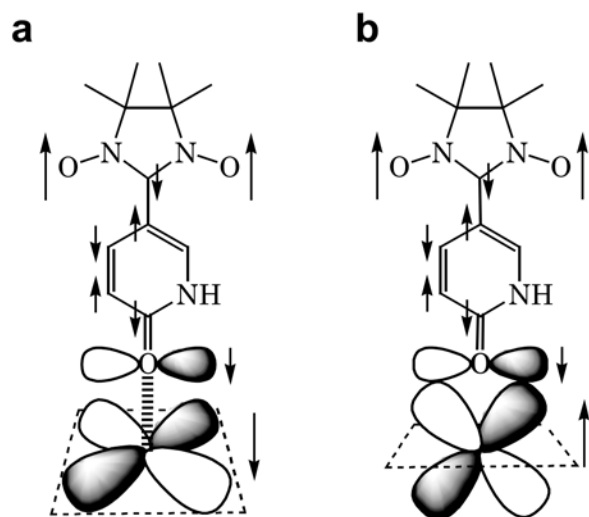


Fig. 9. Schematic illustration of the molecular orbital arrangement relevant to the magnetic exchange interactions in (a) $[\text{Cu}(\text{hfac})_2(\mathbf{1})_2]$ and (b) $[\text{Mn}(\text{hfac})_2(\mathbf{1})_2]$.

Table 1
Crystallographic Parameters

	1	2	[Cu(hfac) ₂ (1) ₂]	[Mn(hfac) ₂ (1) ₂]
Empirical formula	C ₁₂ H ₁₆ N ₃ O ₃	C ₉ H ₁₀ N ₅ O ₂	C ₃₄ H ₃₄ CuF ₁₂ N ₆ O ₁₀	C ₃₄ H ₃₄ MnF ₁₂ N ₆ O ₁₀
Formula weight	250.28	220.21	978.21	969.61
Crystal system	Monoclinic	Monoclinic	Triclinic	Triclinic
<i>a</i> (Å)	8.9193(14)	18.794(13)	7.588(4)	7.4549(4)
<i>b</i> (Å)	19.093(3)	7.637(5)	11.127(3)	11.4901(2)
<i>c</i> (Å)	7.6035(12)	16.993(12)	13.547(3)	13.7931(8)
α (deg)			71.603(16)	69.381(18)
β (deg)	104.919(12)	128.259(9)	82.41(3)	81.77(2)
γ (deg)			76.86(3)	77.39(2)
<i>V</i> (Å ³)	1251.2(3)	1915.2(21)	1054.7(6)	1076.28(17)
Space group	<i>P</i> 2 ₁ / <i>c</i>	<i>C</i> 2/ <i>c</i>	<i>P</i> −1	<i>P</i> −1
<i>Z</i> value	4	8	1	1
<i>D</i> _{calc}	1.329	1.527	1.540	1.496
<i>F</i> (000)	532	920	497	493
No. of reflections	3264	8759	5082	7913
No. of observations	2868	2352	4832	4320
Parameters	169	155	342	341
Temperature (K)	296	80	296	293
<i>R</i> ₁ ^a , <i>wR</i> ₂ ^b (<i>I</i> > 2σ(<i>I</i>))	0.0569, 0.1503	0.0790, — ^c	0.0403, 0.1137	0.0644, 0.1691
<i>R</i> ₁ ^a , <i>wR</i> ₂ ^b (all data)	0.1936, 0.2078	— ^c , 0.1910	0.0707, 0.1265	0.0827, 0.1846
Goodness-of-fit	0.944	1.036	1.059	1.179

^a $R_1 = \sum ||F_o| - |F_c|| / \sum |F_o|$.

^b $wR_2 = [\sum w(F_o^2 - F_c^2)^2 / \sum w(F_o^2)^2]^{1/2}$.

^cData not available.

References

- [1] (a) M. Akazome, S. Suzuki, Y. Shimizu, K. Henmi, K. Ogura, *J. Org. Chem.* 65 (2000) 6917;
(b) É. Boucher, M. Simard, J. D. Wuest, *J. Org. Chem.* 60 (1995) 1408.
- [2] A. Werner, *Ann. Chem.* 386 (1890) 1.
- [3] (a) F. A. Cotton, R. A. Walton, *Multiple Bonds between Metal Atoms*, 2nd ed., Clarendon Press, Oxford (1993), and references cited therein;
(b) R. E. P. Winpenny, *J. Chem. Soc., Dalton Trans.* (2002) 1;
(c) L. S. Hollis, S. J. Lippard, *Inorg. Chem.* 22 (1983) 2600;
- [4] J. M. Rawson, R. E. P. Winpenny, *Coord. Chem. Rev.* 139 (1995) 313.
- [5] (a) J. S. Miller, M. Drillon, Eds., *Magnetism: Molecules to Materials II*, Wiley-VCH, Weinheim (2001);
(b) E. Coronado, P. Delhaes, D. Gatteschi, J. S. Miller, Eds., *Molecular Magnetism : from Molecular Assemblies to the Devices*, Kluwer Academic, Dordrecht (1996);
(c) O. Kahn, *Molecular Magnetism*, VCH, New York (1993).
- [6] (a) H. Sakurai, A. Izuoka, T. Sugawara, *J. Am. Chem. Soc.* 122 (2000) 9723.
(b) J. Cirujeda, M. Mas, E. Molins, F. Lanfranc de Panthou, J. Laugier, J. G. Park, C. Paulsen, P. Rey, C. Rovira, J. Veciana, *J. Chem. Soc., Chem. Commun.* (1995) 709.
- [7] (a) K. Mukai, M. Nuwa, K. Suzuki, S. Nagaoka, N. Achiwa, J. B. Jamali, *J. Phys. Chem. B* 102 (1998) 782;
(b) F. A. Neugebauer, H. Fischer, R. Siegel, *Chem. Ber.* 121 (1988) 815;
(c) R. G. Hicks, M. T. Lemaire, L. Öhrström, J. F. Richardson, L. K. Thompson, Z. Xu, *J. Am. Chem. Soc.* 123 (2001) 7154.
- [8] (a) T. M. Barclay, R. G. Hicks, M. T. Lemaire, L. K. Thompson, Z. Xu, *Chem. Commun.* (2002) 1688;
(d) D. J. R. Brook, S. Fornell, B. Noll, G. T. Yee, T. H. Koch, *J. Chem. Soc., Dalton. Trans.* (2000) 2019.
- [9] (a) M. Ueda, T. Mochida, M. Itou, N. Asanagi, H. Mori, *Inorg. Chim. Acta*, 348C (2003) 123;

- (b) M. Ueda, M. Itou, K. Okazawa, T. Mochida, H. Mori, *Polyhedron*, 24 (2005) 2189.
- [10] T. Mochida, M. Ueda, C. Aoki, H. Mori, *Inorg. Chim. Acta* 335 (2002) 151.
- [11] (a) M. M. Matsushita, A. Izuoka, T. Sugawara, T. Kobayashi, N. Wada, N. Takeda, M. Ishikawa, *J. Am. Chem. Soc.* 119 (1997) 4369;
- (b) E. Hernández, M. Mas, E. Molins, C. Rovira, J. Veciana, *Angew. Chem. Int. Ed.* 32 (1993) 882;
- (c) D. Shiomi, M. Nozaki, T. Ise, K. Sato, T. Takui, *J. Phys. Chem. B* 108 (2004) 16606.
- [12] M. Ueda, T. Mochida, S. Furukawa, H. Suzuki, H. Moriyama, H. Mori, *Mol. Cryst. Liq. Cryst.* 379 (2002) 153.
- [13] L. Vaillancourt, M. Simard, J. D. Wuest, *J. Org. Chem.* 63 (1998) 9746.
- [14] K. Awaga, T. Inabe, Y. Maruyama, T. Nakamura, M. Matsumoto, *Synth. Met.* 56 (1993) 3311.
- [15] (a) Y. Ishimaru, M. Kitano, H. Kumada, N. Koga, H. Iwamura, *Inorg. Chem.* 37 (1998) 2273;
- (b) A. Iino, T. Suzuki, S. Kaizaki, *Dalton Trans.* (2003) 4604.
- [16] M. Lamchen, T. W. Mittag, *J. Chem. Soc.* (1966) 2300.
- [17] C. L. Barr, P. A. Chase, R. G. Hicks, M. T. Lemaire, C. L. Stevens, *J. Org. Chem.* 64 (1999) 8893.
- [18] E. Boucher, M. Simard, J. D. Wuest, *J. Org. Chem.* 60 (1995) 1408.
- [19] Crystal Structure Analysis Package, Molecular Structure Corporation (1999).
- [20] G.M. Sheldrick, Program for the Solution for Crystal Structures; University of Göttingen, Germany (1997).
- [21] ORTEP-3 for Windows, L.J. Farrugia, *J. Appl. Cryst.* 30 (1997) 565.

TOC

